Inorg. Chem. **2008**, *47*, 10810−10812

Observation of Ferroelectricity in Paramagnetic Copper Octacyanomolybdate

Kosuke Nakagawa,[†] Hiroko Tokoro,[†,‡] and Shin-ichi Ohkoshi*[,†]

Department of Chemistry, School of Science, The University of Tokyo, 7-3-1 Hongo, Bunkyo-ku, Tokyo 113-0033, Japan, and PRESTO, JST, 4-1-8 Honcho Kawaguchi, Saitama 332-0012, Japan

Received August 29, 2008

We report the observation of ferroelectricity in a copper octacyanomolybdate-based paramagnet, $Cu_2[Mo(CN)_8]\cdot 8H_2O$ (Cu^{II}, $S = {}^1/_2$; Mo^{IV}, $S = 0$). This compound has a freezing point for the fixation of hydrogen bonding at 150 K. Around this temperature, an enhancement in the ferroelectricity and an increase in the dielectric constant are observed. The ferroelectricity of this system is classified into amorphous ferroelectrics; i.e., the electric poling effect induces an electric polarization. The electric polarization is maintained by the structural local disorder of hydrogen bonding and the three-dimensional CN network. In this ferroelectricity, the crystal structure is a polar group of $C_{\infty v}$ after application of an electric field.

The research of ferroelectricity is one of the attractive issues in the field of material science. The types of ferroelectrics are classified as follows: the displacive-type ferroelectrics (e.g., $BaTiO_3$ and $LiNbO_3$), the order−disorder-type ferroelectrics (e.g., KH_2PO_4 and $NaNO_2$), and the amorphous ferroelectrics[1,2] (e.g., a block copolymer of vinylidene cyanide/vinyl acetate[3]). The category of ferroelectrics of the last one is known as a poled polymer. Recently, also in the field of metal complexes, ferroelectricity has been observed,[4,5] e.g., $Cu_5Cl_9(H_2Quinine)_2$,[4a] $[Mn_3(HCOO)_6](C_2H_5OH)$,[5a] and $Rb_{0.82}Mn[Fe(CN)_6]_{0.94}\cdot H_2O$.[5b] From the viewpoint of discovering new functionalities, the contribution of transition-metal ions (e.g., paramagnetic metal ions) to the ferroelectric property is very attractive for chemists, physicists, and materials scientists. A cyano-bridged bimetal assembly[6] is a good candidate the preparation of a ferroelectric metal−complex assembly because the $C{\equiv}N^-$ group potentially has a large electric dipole moment of 3.5 D.[2] In this work, we focus on copper octacyanomolybdate, $Cu^{II}_2[Mo^{IV}(CN)_8]\cdot 8H_2O$ (Cu^{II}, $S = {}^1/_2$; Mo^{IV}, $S = 0$). This compound is known to be a class II type mixed-valence compound that shows paramagnetism and a photoinduced charge transfer from Mo^{IV} to Cu^{II} sites.[7] Herein, we report the ferroelectric and dielectric properties of $Cu^{II}_2[Mo^{IV}(CN)_8]\cdot 8H_2O$ and discuss its mechanism.

The target compound was prepared using a previously reported method.[7d] An aqueous solution (0.2 mol dm^{-3}) of $CuCl_2$ was reacted with an aqueous solution of $K_4[Mo(CN)_8]$

* To whom correspondence should be addressed. E-mail: ohkoshi@chem.s.u-tokyo.ac.jp.
† The University of Tokyo.
‡ PRESTO, JST.

(1) Lines, M. E.; Glass, A. M. *Principles and Applications of Ferroelectrics and Related Materials*; The International Series of Monographs on Physics; Clarendon Press: Oxford, U.K., 1977.
(2) *Ferroelectric Polymers: Chemistry, Physics, and Applications*; Nalwa, H. S., Ed.; Marcel Dekker, Inc.: New York, 1995.
(3) (a) Gilbert, H.; Miller, F. F.; Averill, S. J.; Schmidt, R. F.; Stewart, F. D.; Trumbull, H. L. *J. Am. Chem. Soc.* **1954**, *76*, 1074. (b) Tasaka, S.; Miyasato, K.; Yoshikawa, M.; Miyata, S.; Ko, M. *Ferroelectrics* **1984**, *57*, 267. (c) Wang, T. T.; Takase, Y. *J. Appl. Phys.* **1987**, *62*, 3466.
(4) (a) Zhao, H.; Qu, Z. R.; Ye, Q.; Abrahams, B. F.; Wang, Y. P.; Liu, Z. G.; Xue, Z.; Xiong, R. G.; You, X. Z. *Chem. Mater.* **2003**, *15*, 4166. (b) Qu, Z. R.; Zhao, H.; Wang, Y. P.; Wang, X. S.; Ye, Q.; Li, Y. H.; Xiong, R. G.; Abrahams, B. F.; Liu, Z. G.; Xue, Z. L.; You, X. Z. *Chem. Eur. J.* **2004**, *10*, 53.
(5) (a) Cui, H. B.; Wang, Z.; Takahashi, K.; Okano, Y.; Kobayashi, H.; Kobayashi, A. *J. Am. Chem. Soc.* **2006**, *128*, 15074. (b) Ohkoshi, S.; Tokoro, H.; Matsuda, T.; Takahashi, H.; Irie, H.; Hashimoto, K. *Angew. Chem., Int. Ed.* **2007**, *46*, 3238. (c) Li, X. L.; Chen, K.; Liu, Y.; Wang, Z. X.; Wang, T. W.; Zuo, J. L.; Li, Y. Z.; Wang, Y.; Zhu, J. S.; Liu, J. M.; Song, Y.; You, X. Z. *Angew. Chem., Int. Ed.* **2007**, *46*, 6820. (d) Wang, G. X.; Han, G. F.; Ye, Q.; Xiong, R. G.; Akutagawa, T.; Nakamura, T.; Chan, P. W. H.; Huang, S. D. *Dalton Trans.* **2008**, 2527. (e) Chen, C. T.; Suslick, K. S. *Coord. Chem. Rev.* **1993**, *128*, 293. (f) Okubo, T.; Kawajiri, R.; Mitani, T.; Shimoda, T. *J. Am. Chem. Soc.* **2005**, *127*, 17598.
(6) (a) Ferlay, S.; Mallah, T.; Ouahès, R.; Veillet, P.; Verdaguer, M. *Nature* **1995**, *378*, 701. (b) Hatlevik, Ø.; Buschmann, W. E.; Zhang, J.; Manson, J. L.; Miller, J. S. *Adv. Mater.* 1999, *11*, 914. (c) Holmes, S. M.; Girolami, G. S. *J. Am. Chem. Soc.* **1999**, *121*, 5593. (d) Margadonna, S.; Prassides, K.; Fitch, A. N. *J. Am. Chem. Soc.* **2004**, *126*, 15390. (e) Kaye, S. S.; Long, J. R. *J. Am. Chem. Soc.* **2005**, *127*, 6506. (f) Varret, F.; Boukheddaden, K.; Codjovi, E.; Goujon, A. *Hyperfine Interact.* **2005**, *165*, 37. (g) Moore, J. G.; Lochner, E. J.; Ramsey, C.; Dalal, N. S.; Stiegman, A. E. *Angew. Chem., Int. Ed.* **2003**, *42*, 2741. (h) Pejaković, D. A.; Manson, J. L.; Miller, J. S.; Epstein, A. J. *Phys. Rev. Lett.* **2000**, *85*, 1994. (i) Coronado, E.; Giménez-López, M. C.; Levchenko, G.; Romero, F. M.; García-Baonza, V.; Milner, A.; Paz-Pasternak, M. *J. Am. Chem. Soc.* **2005**, *127*, 4580.
(7) (a) Ohkoshi, S.; Machida, N.; Zhong, Z. J.; Hashimoto, K. *Synth. Met.* **2001**, *122*, 523. (b) Rombaut, G.; Verelst, M.; Golhen, S.; Ouahab, L.; Mathonière, C.; Kahn, O. *Inorg. Chem.* **2001**, *40*, 1151. (c) Herrera, J. M.; Marvaud, V.; Verdaguer, M.; Marrot, J.; Kalisz, M.; Mathonière, C. *Angew. Chem., Int. Ed.* **2004**, *43*, 5468. (d) Ohkoshi, S.; Tokoro, H.; Hozumi, T.; Zhang, Y.; Hashimoto, K.; Mathonière, C.; Bord, I.; Rombaut, G.; Verelst, M.; Moulin, C. C. D.; Villain, F. *J. Am. Chem. Soc.* **2006**, *128*, 270.

10.1021/ic8016563 CCC: $40.75
Published on Web 10/29/2008

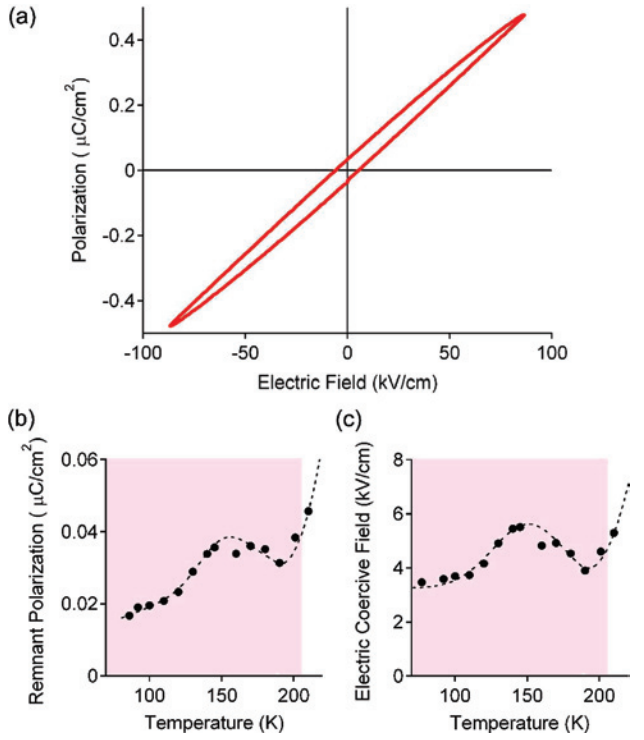

Figure 1. Ferroelectric properties of $Cu_2[Mo(CN)_8]\cdot 8H_2O$. (a) Polarization versus electric field curve ($P-E$ hysteresis loop) at 145 K. Temperature dependence of (b) the remnant polarization and (c) the electric coercive field values upon application of ±86 kV cm^{-1}. Dotted lines are to guide the eye. In the red area, the leakage current is perfectly suppressed.

(0.2 mol dm^{-3}) to yield a precipitate, which was filtered and dried to give a powder sample. Elemental analysis showed that the formula was $Cu_2[Mo(CN)_8]\cdot 8H_2O$.[8] In the IR spectra at room temperature, the CN stretching frequency of $Cu^{II}-NC-Mo^{IV}$ was observed at 2165 cm^{-1}. The superconducting quantum interference device measurement confirmed that this compound showed paramagnetism due to Cu^{II} in the entire temperature range between 5 and 300 K. The electric polarization (P) versus the applied electric field (E) plots were measured using an electric polarization hysteresis meter. The dielectric constant (ε) was measured using an LCR meter. The sample temperature was controlled by our laboratory-made liquid-N_2 system. Details to prepare samples for the P vs E plots and the ε measurement are described in the Supporting Information.

Figure 1a shows the P vs E plots for the present compound when a field up to ±86 kV cm^{-1} was applied. The P vs E curve of the compound at 145 K shows a $P-E$ hysteresis loop with a remnant electric polarization (P_r) of 0.036 μC cm^{-2} and an electric coercive field (E_c) of 5.5 kV cm^{-1}. To confirm the ferroelectrics, the leakage current measurement is necessary because a mouth-shaped $P-E$ curve easily appears as a result of the leakage current. Figure 2a shows the current versus E plots, and Figure 2b shows the current versus temperature (T) plots, respectively. Below 210 K, the electric current was extremely low (less than 10^{-10} A cm^{-2} of the measurement limitation). Hence, the observed hysteresis loop below 200 K is clearly due to ferroelectricity. In contrast, above 210 K, because the contribution of the leakage current was observed, we could not judge the ferroelectricity. The origin of the leakage current is due to the conductivity on the surface of the microcrystals of the sample. Hence, we here discuss only the $P-E$ plots below 210 K. Parts b and c of Figure 1 show the P_r vs T and the E_c vs T plots, respectively, and indicate that the maximum values ($P_{r,max}$ and $E_{c,max}$) are around 150 K.

(8) Elemental analysis, which was confirmed by inductively coupled plasma mass spectroscopy and standard microanalytical methods, demonstrated that the formula was $Cu_2[Mo(CN)_8]\cdot 8H_2O$. Elem anal. Calcd: Cu, 22.09; Mo, 16.68; C, 16.70; N, 19.48. Found: Cu, 21.91; Mo, 16.60; C, 16.49; N, 18.94.

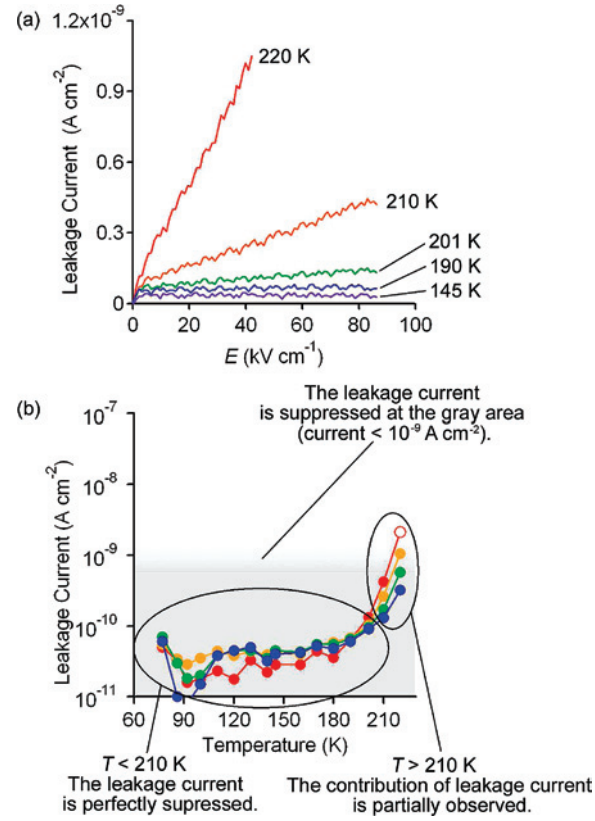

Figure 2. Leakage current in the $Cu_2[Mo(CN)_8]\cdot 8H_2O$ system. (a) Leakage current vs applied electric field (E) at 145 (purple), 190 (blue), 201 (green), 210 (orange), and 220 (red) K. (b) Temperature dependence of the leakage current at various E values [11 (blue), 22 (green), 43 (orange), and 86 (red) kV cm^{-1}]. The red open circle of 86 kV cm^{-1} was estimated by the extrapolation of the current versus E plots at 220 K.

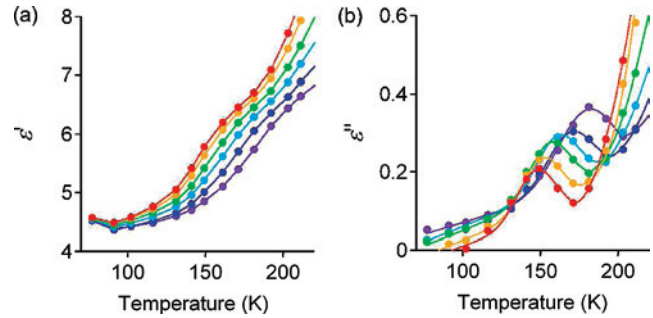

Figure 3. Temperature dependence of the (a) real (ε') and (b) imaginary (ε'') parts of the dielectric constant of $Cu_2[Mo(CN)_8]\cdot 8H_2O$ upon application of ±25 V cm^{-1}: 0.2 (red), 0.5 (orange), 2 (green), 7 (light blue), 30 (blue), and 200 (purple) kHz.

Parts a and b of Figure 3 show the temperature dependence of the real (ε') and imaginary (ε'') parts of ε. In the ε'' vs T plots, the maximum value (ε_{max}'') was observed at 150 K

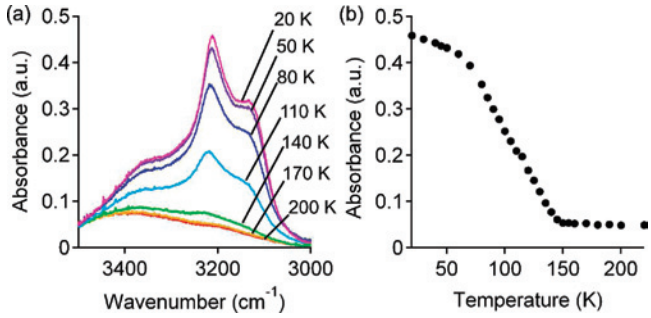

Figure 4. Temperature dependence of the (a) IR spectra and (b) peak intensities at 3210 cm^{-1} in $Cu_2[Mo(CN)_8]\cdot 8H_2O$.

with a low electric frequency of 0.2 kHz. As the frequency increased, the peak position of ε_{max}'' shifted to higher temperature, i.e., 150 K (0.2 kHz) → 180 K (200 kHz). Shoulder peaks were observed in the ε' vs T plots at corresponding temperatures. The increase in ε'' above 200 K is due to the charge polarization on the surface of the microcrystals of the sample. In fact, a leakage current was also observed above 210 K, as mentioned above.

To investigate the origin of electric polarization, the temperature dependence of the IR spectra of the present compound was measured. Figure 4a shows the temperature dependence in the range of 3000−3500 cm^{-1}. Below 150 K, new peaks rapidly appeared around 3200 cm^{-1} (Figure 4b), which were assigned to the OH stretching modes due to fixation of hydrogen bonds between the ligand water molecules on Cu^{II} and zeolitic water molecules in the interstitial sites. That is, the freezing point (T_g) of hydrogen bonding is around 150 K in this system.

The powder X-ray diffraction (XRD) pattern showed a broad peak pattern (Figure S1 in the Supporting Information), suggesting that the crystal structure is nearly amorphous and that local disorder exists inside the compound. As for the local coordinates around Cu^{II} and Mo^{IV}, the results of wide-angle X-ray scattering and X-ray absorption spectroscopies[7d] indicate that Cu^{II} is connected to four cyano nitrogens and two oxygens from water molecules, while Mo^{IV} is connected to eight cyano carbons (Figure 5).

On the basis of the results of ferroelectric, dielectric, and structural measurements, we discuss the mechanism of the observed ferroelectricity. The existence of ε_{max}'' around 150 K suggests that the mobility of the electric dipole moment increases in this temperature region. Because the temperature of ε_{max}'' corresponds to those of $P_{r,max}$ and $E_{c,max}$ and T_g of hydrogen bonding also exists around 150 K, the fixation of hydrogen bonding is clearly related to the driving force of the observed ferroelectricity. The dependence of the shift in the ε_{max}'' position on the

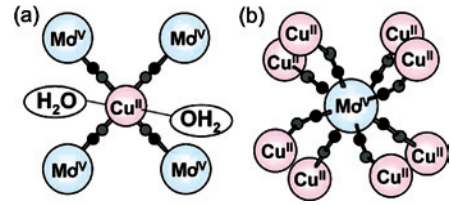

Figure 5. Schematic illustration of the local structures of (a) Cu and (b) Mo in $Cu_2[Mo(CN)_8]\cdot 8H_2O$.

frequency implies a short-range order of electric polarization, which is usually observed in poled polymers of amorphous ferroelectrics.[2,3] In these types of ferroelectrics, the crystal structure is a polar group of $C_{\infty v}$ after the application of an electric field. In fact, our compound also has a near-amorphous structure. Hence, the local electric dipole moment is aligned as a result of the electric poling effect to produce electric polarization, which remains as remnant electric polarization even after removal of the external electric field due to the structural flexibility of the hydrogen bonds and CN network.

In summary, we observed ferroelectricity using a copper octacyanomolybdate-based paramagnet, which has an amorphous structure and a freezing point for the fixation of hydrogen bonding at 150 K. Around this temperature, an enhancement in the ferroelectricity and an increase in the dielectric constant are observed. The electric poling effect induces electric polarization in this system, which is maintained by the structurally local disorder due to hydrogen bonding and the three-dimensional CN network. Usually, ferroelectrics in inorganic crystals are classified into displacive -type ferroelectrics or order−disorder-type ferroelectrics. However, the ferroelectricity in the present compound is explained by the mechanism for amorphous-type ferroelectrics.

Acknowledgment. The present research was supported in part by a Grant for the Global COE Program "Chemistry Innovation through Cooperation of Science and Engineering" and technology and a Grant-in-Aid for Young Scientists (S) from the JSPS, Inamori Foundation, The Kurata Memorial Hitachi Science and Technology Foundation, and The Murata Science Foundation.

Supporting Information Available: Information related to the detailed sample procedure for the P vs E plots and the ε measurement and the XRD pattern of $Cu_2[Mo(CN)_8]\cdot 8H_2O$. This material is available free of charge via the Internet at http://pubs.acs.org.

IC8016563